

Theoretical Investigation of Passively Mode-locked Quantum Dot Laser

Aref Rasoulzadehzali¹, Mohammad Kazem Moravvej-farshi¹, Javad Rahimi¹, Mohammad Hassan Yavari²

¹Faculty of Electrical and Computer Engineering, Tarbiat Modares University, Tehran 14117-13116, Iran.

Aref.rasoulzadehzali@modares.ac.ir, farshi_k@modares.ac.ir, J.rahimi@modares.ac.ir

²Faculty of Engineering, Shahed University, Tehran, Iran, mh.yavari@shahed.ac.ir

Abstract—Using models based on delay differential equation (DDE) and finite difference traveling wave (FDTW), we have obtained the characteristics of passively quantum dot mode-locked lasers (QD-MLLs). By manipulating DDE, it is shown that by an increase in the saturable absorber's (SA) reverse bias, the pulse width decreases while the stability of the pulse time domain response decreases. Besides, the range of enhancement factor to have a stable pulse decreases as well. Moreover, DDE model shows that by controlling unsaturated gain and loss ratio harmonic mode locking is achievable. Finally, FDTW model is used to investigate the spatio-temporal features of QD-MLLs. Although this method substantially increases the simulation complexity due to the complex rate equations alongside with two dimensional simulation grid, it provides a more comprehensive simulation tool for analysing the device.

Keywords—component; Delay differential equation model (DDE); Finite difference travelling wave model (FDTW); saturable absorber (SA); quantum dot mode-locked laser.

I. INTRODUCTION

Recently, due to the superior performances, quantum dot mode-locked lasers (QD-MLLs) have been considered as alternatives to quantum well mode-locked lasers (QW-MLLs). The important goal of the mode locking in semiconductor lasers is to generate stable short pulses. Distinctive properties of self-assembled QD (SA-QD) active regions, such as low values of linewidth enhancement factors (Henry's factor), unsaturated gain and absorption make QDLs considerably efficient compared to its counterparts such as bulk and quantum well lasers [1-4].

Different modelling techniques such as finite difference travelling wave (FDTW) model and delay differential equation (DDE) model have been developed to analyze semiconductor mode-locked lasers and especially QDMLLs [5, 6]. FDTW model consider spatial distribution of carriers and electric field amplitude without assuming unidirectional lasing in a ring cavity (as assumed in DDE model). It also computationally expensive and needs enormous computation to simulate laser behavior. On the other hand, using delay differential equation (DDE) method to model passive mode-locked laser in various operating conditions is a powerful tool to simulate laser performance [6-9]. Besides, DDE model can guide us to design the laser and anticipate clearly its operation. DDE model uses 9

parameters in modelling of the device that can be extracted from measurable quantities. So, DDE based simulations are very time efficient and need lower computation than FDTW model. In this paper we will follow the two FDTW and DDE approach to simulate laser behavior. But as we will observe, DDE model needs less computation and is simpler than FDTW model.

II. USING DELAY DIFFERENTIAL EQUATION (DDE) MODEL TO SIMULATE QDMLL

The device simulated by using DDE model with a 1mm absorber section and 7mm gain section, is similar structure proposed in [8, 9] with 8 stacks dots in well structure which can be grown by molecular beam epitaxy (MBE).

DDE model firstly was introduced by Vladimirov and Turaev [6, 7] which was derived from coupled partial differential equations (PDE) based on FDTW model which describe the optical wave and carrier densities in the cavity including gain and absorber sections [5, 8, 9]:

$$\frac{\partial E(t, z)}{\partial z} + \frac{1}{v} \frac{\partial E(t, z)}{\partial t} = \frac{g_r \Gamma_r}{2} (1 - i\alpha_r) \left[N_r(t, z) - N_r^{tr} \right] \times E(z, t), \quad (1)$$

$$\frac{\partial N_r(t, z)}{\partial z} = J_r - \gamma_r N_r(t, z) - v g_r \Gamma_r \left[N_r(t, z) - N_r^{tr} \right] \times |E(z, t)|^2. \quad (2)$$

In the above mentioned equations, $E(t, z)$ describes complex optical field in the cavity. Subscript $r=q$ (or $r=g$) relates to absorber (gain) section. The parameters g_r , Γ_r , α_r , and γ_r are differential gains, transverse modal fill factor, linewidth enhancement factor, and carrier density relaxation rates in the corresponding gain and absorber sections, respectively. The parameter J_r indicates the injected current density in the corresponding absorption and gain sections. v is constant light group velocity, in both gain and absorber sections. Using the transformation described in [6, 7, 9], the two dimensional (spatio-temporal) equations in FDTW model can be converted to a one dimensional (temporal) system of DDE equations [6-9]:

$$\frac{dA}{dt} = -\gamma A(t) + A(t-T)\gamma\sqrt{\kappa}e^{\left\{0.5\left[(1-i\alpha_g)G(t-T)-(1-i\alpha_q)Q(t-T)\right]\right\}} \quad (3)$$

$$\frac{dG}{dt} = g_0 - \Gamma G(t) - e^{-Q(t)}(e^{G(t)} - 1) |A(t)|^2 \quad (4)$$

$$\frac{dQ}{dt} = q_0 - Q(t) - s(1 - e^{-Q(t)}) |A(t)|^2 \quad (5)$$

where, the delay parameter, T , is normalized roundtrip time. A , G , and Q are optical field, saturable gain, and saturable loss, respectively. α_q and α_g are linewidth enhancement factors in the absorber and gain sections, respectively. Linear cavity loss is depicted by κ . The carrier relaxation ratio or Γ is the ratio of the absorption relaxation time to gain relaxation time, $\Gamma = \tau_{abs}/\tau_{gain}$. Saturation parameter s , can be defined as the ratio of differential absorption to differential gain. q_0 and g_0 represent the unsaturated absorption and gain, respectively [8, 9]. In order to have fundamental mode-locking we follow the stability analysis of [6] and use its stability criteria. The resultant criterion to have stable mode locking is: $q_0 = mg_0$ which m corresponds to the slope of a line in the $q_0 - g_0$ plane and clearly should be chosen correctly to ensure fundamental mode locking.

A. Results

The device parameters are extracted by segmented contact method (SCM) at 20°C and three different bias conditions for saturable absorber (SA) which are listed in Table I [8, 9]. The pre-mentioned DDE equations which define the model (equations (3), (4), (5)) are solved over two thousand round trip times to settle transient condition. Fig. 1(a) and 1(b) shows time domain simulation of the pulse intensity for 3V SA reverse bias condition. It is worth noting that by increasing the bias voltage, the pulse time domain response will be more unstable, though it may decrease pulse width.

A parameter that can play crucial role in the device performance is the ratio of unsaturated gain and loss parameters (or m). One can achieve higher pulse repetition rate by engineering this parameter (m) [8, 9]. For instance, it can be shown that by gradually increasing m , one can achieve harmonic mode locking. As Fig. 2 (a) and (b) shows, onset of pulse can be predicted for $m=0.5$. The values used in simulation are listed in Table I (for 3V reverse biased condition). As the ratio of unsaturated gain to loss (m) increases the intensity of the pulse increases and the laser continues to work in fundamental mode locking state.

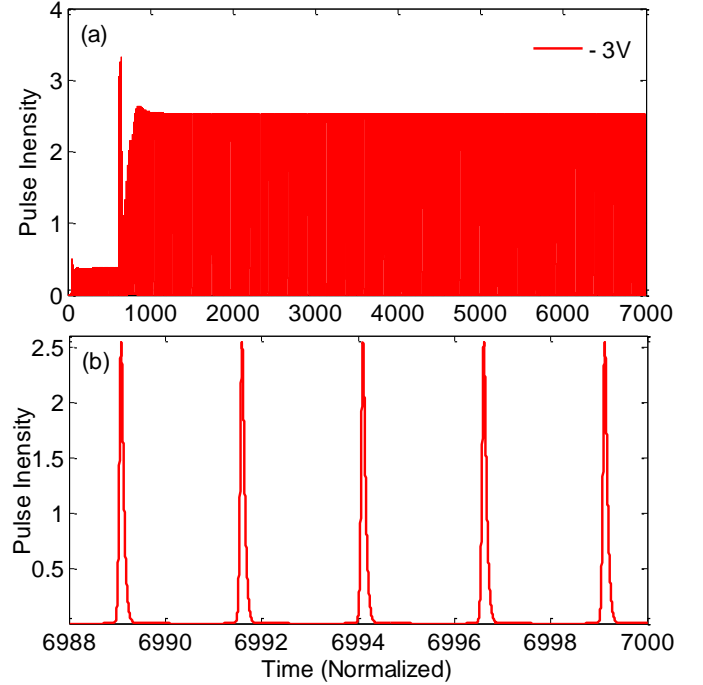


Figure 1(a) Transient and steady state response of QDMLL for -3V absorber bias and for $\alpha_g, q = 1.8$. (b) The zoomed pulse shape

Slightly after $m = g_0/q_0 = 7/8$ the laser starts entering to second harmonic mode locking (as depicted in Fig. 2(b)) regime which two pulses are in the cavity per roundtrip. Fig. 3 (a) and (b) depicts results of mode locking behavior by increasing m values for 5V reverse biased condition for SA. Fig. 3(a) shows details of time domain behavior of mode locking for -5V bias. The simulation parameters seed the simulation are listed in the first column of Table I. The onset of pulse can be predicted for $m=1/8$. In this condition the laser operates in fundamental mode locking regime. By increasing the m to $5/8$, second harmonic mode locking starts emerging and repetition rate doubles as well (Fig. 3(b)). It is important to note that by increasing m value further (to $m < 1$), the onset of third harmonic mode locking arises. These results correspond to those achieved in [8, 9].

Table I: Parameters used in the device simulation over different bias condition and at 20°C [8, 9].

Parameters	-5 V	-3 V
T	6.67	5
$G(0)$	4.18	4.18
$Q(0)$	4.55	3.20
α_g	0.5	0.2
α_q	0.5	0.2
κ	0.55	0.55
γ	41.10	39.15
Γ	0.08	0.08
s	6.90	4.65

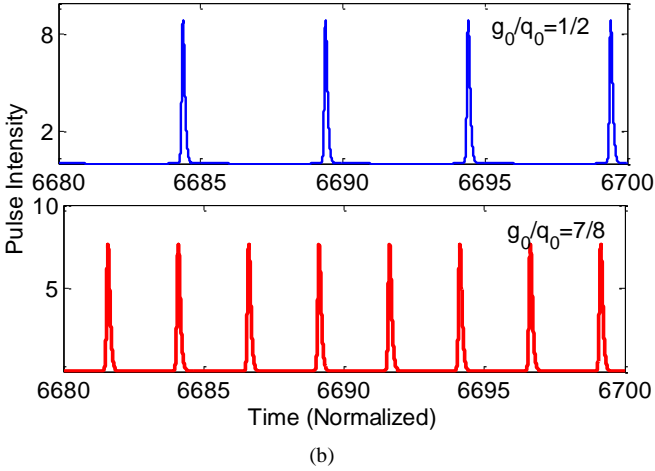
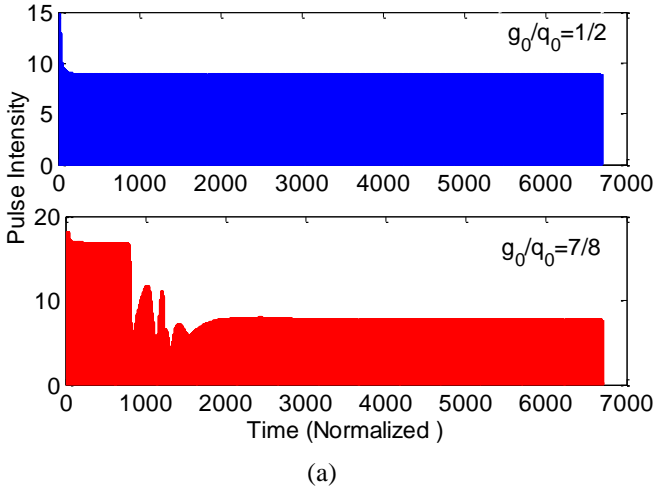


Figure 2(a) Pulse intensity for different unsaturated gain to absorption ratio (m) for -3V bias condition. (b) The corresponding zoomed pulse shapes.

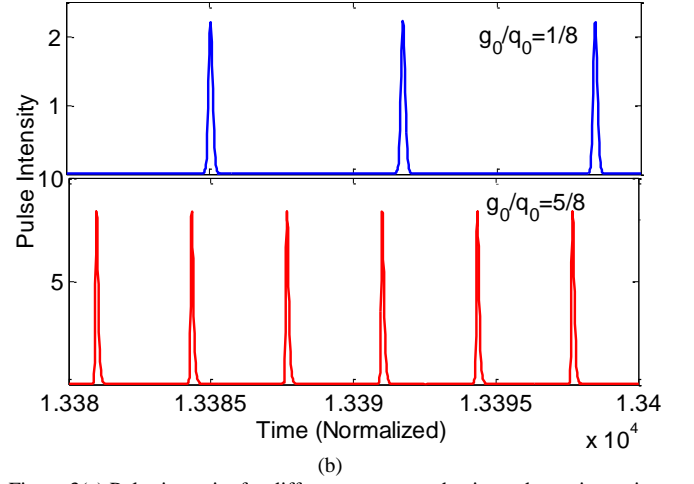
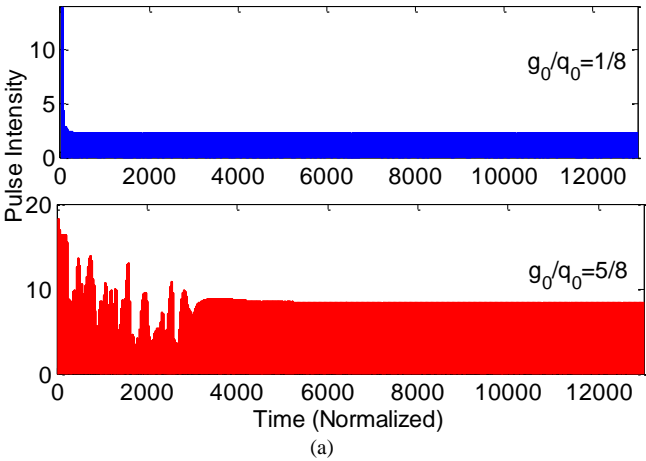


Figure 3(a) Pulse intensity for different unsaturated gain to absorption ratio (m) for -5V bias condition. (b) The corresponding zoomed pulse shapes.

II. USING FINITE DIFFERENCE TRAVELLING WAVE (FDTW) MODEL TO SIMULATE QDMLL

The device simulated in this paper by using FDTW model is 1mm laser cavity including 0.1mm absorption and 0.9mm gain sections, similar to the structure proposed in [10, 11]. Two dimensional numerical grid (temporal and spatial grid) is used to model spatio-temporal evolution of the counter propagating fields in the two section laser cavity [10, 11]. The coupled formalism and two dimensional grid means that to increase the resolution of the results, we should increase the steps (number of grids) which can increase our computation and simulation time as well. Furthermore, some terms in the rate equations are itself described by other equations which indicates that one faces vastness of parameters to use FDTW model for simulation two section laser [9]. As a result, compared with DDE model, FDTW method is complex and needs great numerical calculation. Besides, FDTW model takes all details of the equations into account and is more accurate than DDE model. A simplified flowchart of FDTW simulation is depicted in Fig. 4. The parameters used in simulation are given in Table II.

The governing travelling wave equations of two counter propagating optical field in the two section cavity is [10, 11]:

Table II: Parameters used in FDTW model [10, 11]

Symbol	Quantity	Value
λ_0	Central wavelength	1.3 μm
n_g	Group refractive index	3.75
L	Total length	1mm
l_{SA}	SA length	100 μm
δ	Static detuning	0 cm^{-1}
α	Internal absorption	5 cm^{-1}
α_H	Henry factor	2
g'	Differential gain/absorption	40/200 cm^{-1}
τ_{gs}	GS relaxation rate	1ns
τ_{es}	ES relaxation rate	1ns
τ_{cr}	CR relaxation rate	1ns
$\tau_{es \rightarrow gs}$	ES to GS Transition time	2ps
$\tau_{gs \rightarrow es}$	GS to ES Transition time	5ps
$\tau_{cr \rightarrow es}^{-1}$	CR to ES Transition rate (SA)	0
$\tau_{cr \rightarrow es}$	CR to ES Transition rate (G)	5ps
$\tau_{es \rightarrow cr}$	ES to CR Transition rate (SA)	$18e^{V_{sa}/2}$ ps
$\tau_{es \rightarrow cr}$	ES to CR Transition rate (G)	80ps
Γ	Transversal confinement factor	0.075
r_0	Left facet reflectivity	$\sqrt{0.95}$
r_L	Right facet reflectivity	$\sqrt{0.3}$

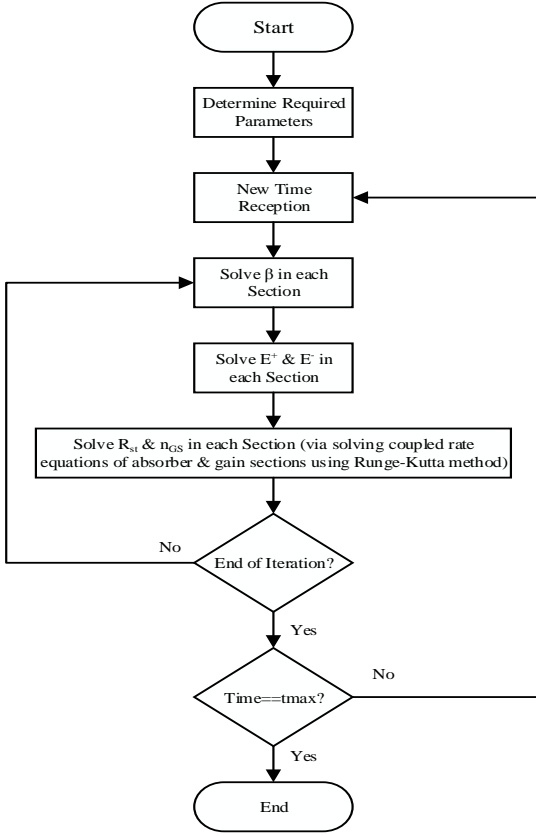


Figure 4. Flowchart of FDTW simulation steps.

$$\frac{\partial}{\partial t} E^\pm(z, t) = \frac{c}{n_g} \left(\mp \frac{\partial E^\pm}{\partial z} - i\beta E^\pm \right) + F_{sp}^\pm, \quad (6)$$

with boundary condition at two facets ($z=0, L$):

$$E^-(L, t) = r_L E^+(L, t), \quad E^+(0, t) = r_0 E^-(0, t). \quad (7)$$

Here, c is light speed in vacuum, n_g is group refractive index, F_{sp}^\pm describes spontaneous emission noise, $r_{0,L}$ stands for laser facets reflectivity. Assuming that the propagation factor (β) depends only on n_{gs} (ground state occupation probability), it can be formulated as [10, 11]:

$$\beta(n_{gs}) = \frac{(i - \alpha_H)}{2} g'(2n_{gs} - 1) - i\frac{\alpha}{2} + \delta, \quad (8)$$

wherein α_H , g' , α , and δ represent linewidth enhancement factor, differential gain/absorption, internal loss, and detuning from reference wavelength. It is worth noting that the frequency dependence of gain profile is neglected in this work. So, material dispersion operator in our simulation is assumed to be zero. Carrier rate equations between different states (ground state (GS), excited state (ES), and carrier reservoir (CR) of quantum dots) for two absorber and gain sections are described in [10].

Carrier rate equations in the gain section can be described as [10, 11]:

$$\begin{aligned} \frac{dn_{gs}(n, z)}{dt} &= -\frac{n_{gs}}{\tau_{gs}} - R_{st}(n_{gs}, E) + 2R_{es,gs} \\ \frac{dn_{es}(n, z)}{dt} &= -\frac{n_{es}}{\tau_{es}} - R_{es,gs} + R_{cr,es} \\ \frac{dn_{cr}(n, z)}{dt} &= \frac{I}{e\theta_I} - \frac{n_{cr}}{\tau_{cr}} - 4R_{cr,es} \end{aligned} \quad (9)$$

which $n_{es,gs}$ and n_{cr} are occupation probabilities of corresponding states. $R_{cr,es}$ and $R_{es,gs}$ are carrier recombination rates which are fully described in [10] as follows:

$$\begin{aligned} R_{cr,es} &= \frac{(1 - n_{es})n_{cr}}{4\tau_{cr \rightarrow es}} - \frac{n_{es}}{\tau_{es \rightarrow cr}} \\ R_{es,gs} &= \frac{(1 - n_{gs})n_{es}}{\tau_{es \rightarrow gs}} - \frac{(1 - n_{es})n_{gs}}{2\tau_{gs \rightarrow es}}. \end{aligned} \quad (10)$$

Here, θ_I and R_{st} are respectively scaling factor and stimulated emission rate which are fully described in [10].

Carrier rate equations in the saturable absorber (SA) section ($0 < z < l_{SA}$) can be described as [10, 11]:

$$\begin{aligned} \frac{dn_{gs}(n, z)}{dt} &= -\frac{n_{gs}}{\tau_{gs}} - R_{st}(n_{gs}, E) + 2R_{es,gs} \\ \frac{dn_{es}(n, z)}{dt} &= -\frac{n_{es}}{\tau_{es \rightarrow cr}} - R_{es,gs} \end{aligned} \quad (11)$$

B. Simulation Results

Fig. 5(a) and 5(b) show numerical simulation of pulse intensity using FDTW model for different injection currents. At low injection currents (above laser threshold for $I=35$ mA) the laser operates in Q-switching regime, as shown in Fig. 5(b). Furthermore, by increasing the injection currents, to $I=45, 65, 80, 100,$ and 120 mA, as Fig. 5(a) shows, laser enters fundamental mode-locking regime and generates stable pulse shapes. The peak power of the emitted pulse for different currents is almost constant. By increasing injection current, the pulse shapes experience some type of asymmetry. The more

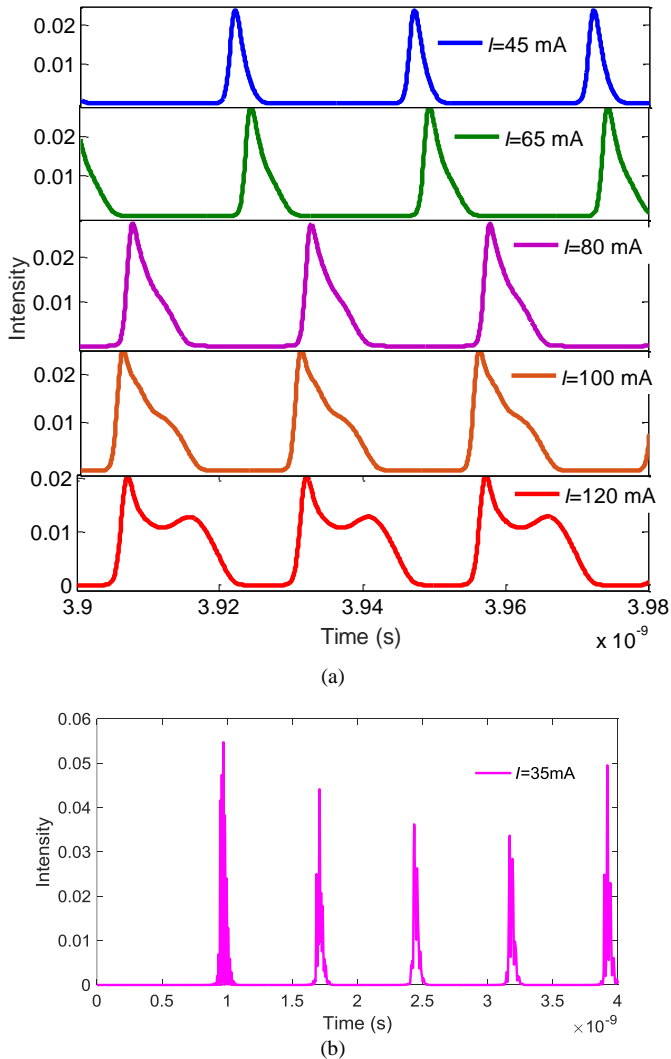


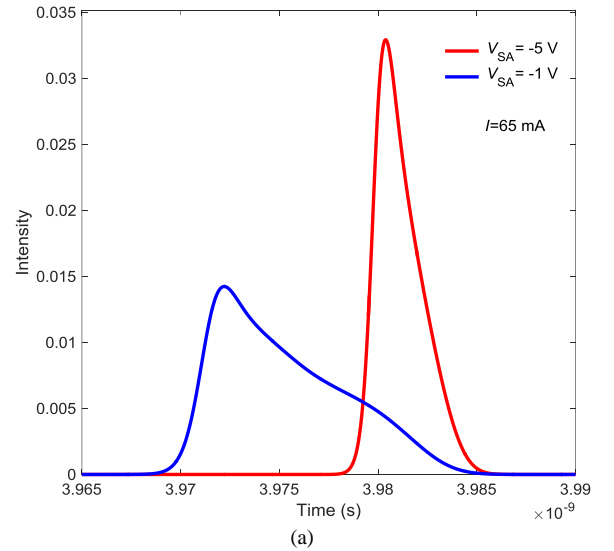
Figure 5 (a) Pulse intensity for different injection currents including $I=45, 65, 80, 100,$ and 120 mA. (b) Pulse intensity for $I=35$ mA

the injected current (to the gain section) is, the less symmetric the pulse is. It is also important to note that the pulse width increases and experiences a broad trailing edge plateau (TEP) as the injected current increases [10, 11]. Finally for larger injection currents, the laser switches to continuous wave mode regime.

One of the major and important parameters that can affect the pulse shape of mode-locked laser, is the reverse voltage bias of saturable absorber (SA). We assume that all the transition rates are independent of voltage (V_{SA}) except $\tau_{es \rightarrow gs}$.

It is assumed that $\tau_{es \rightarrow cr}$ has exponential dependence on SA absorber reverse bias (V_{SA}). Fig. 6(a) and 6(b) show the effects of SA reverse bias voltage on the pulse shape for two different injected currents. As shown, the pulse width (FWHM) increases as the SA bias increases. For instance, for $I=65$ mA, the pulse width for $V_{SA}=-5$ V is narrower than the pulse width for $V_{SA}=-1$ V. Besides, the pulse intensity for $V_{SA}=-1$ V is less than the pulse intensity for $V_{SA}=-5$ V. This trend also can be observed in Fig. 6(b). For $I=100$ mA, the pulse intensity for $V_{SA}=-5$ V is the highest. On the other hand the pulse width for $V_{SA}=-2$ V is the broadest. By increasing the SA reverse bias, the transition time from ES to CR decrease and by accelerating the carrier transition from ES to CR, the occupation probability of GS decreases. So this phenomenon causes the SA to saturate in a narrow time interval which makes the pulse width narrow. On the other hand, by increasing SA reverse bias, the absorption of the SA increases and this effect allows the modes with same phase to contribute the pulse intensity and filters the modes which are out of phase.

In conclusion, DDE model is a very efficient model that can predict the QD-MLL behavior with limited parameters which can be achieved by segmented contact method (SCM). Using this model, we can easily simulate steady state and transient behavior of the device under different conditions. As can be seen, the accuracy of the results is acceptable. It is shown that by decreasing the absorber reverse voltage, the acceptable range of enhancement factor to have a stable pulse increases.



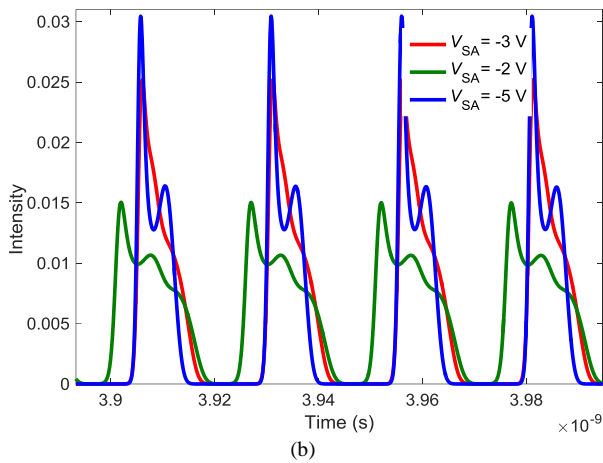


Figure 6(a). Pulse intensity for two different bias condition of SA, but for a same injection current ($I=65\text{mA}$). (b) Pulse intensity for three different bias condition of SA, but for a same injection current ($I=100\text{mA}$)

Moreover, by engineering m parameter one can achieve higher repetition rate in the cavity for different gain currents. It is worth mentioning that by further increasing the m parameter, the pulse shape may experience some instabilities and chaotic behavior. On the other hand, we show that two dimensional numerical grid (time and space grid) which used to solve the FDTW model makes the model more complex. Also, the terms describing the laser's rate equations are complex and two dimensional (spatio-temporal) grid increases numerical computation and simulation time. As a result, compared with DDE model FDTW method needs great numerical computation, though FDTW model takes all details into account and is more accurate than DDE model. It is shown that by increasing the current and decreasing SA reverse voltage, pulse width increases.

REFERENCES

- [1] E. U. Rafailov, M. A. Cataluna, E.A. Avrutin, *Ultrafast Lasers Based on Quantum Dot Structures*, John-Wiley, 2011.
- [2] E. U. Rafailov, M. A. Cataluna, and W. Sibbett, "Mode-locked quantum-dot lasers," *Nature Photon.*, Vol. 1, No. 7, pp. 395–401, 2007.
- [3] M. G. Thompson, A. R. Rae, M. Xia, R. V. Penty, and I. H. White, "InGaAs quantum-dot mode-locked laser diodes", *IEEE J. Sel. Topics Quantum Electron.*, Vol. 15, No. 3, pp. 661-672, 2009.
- [4] G. T. Liu, A. Stintz, H. Li, K. J. Malloy and L. F. Lester, "Extremely low room-temperature threshold current density diode lasers using InAs dots in $\text{In}_{0.15}\text{Ga}_{0.85}\text{As}$ quantum well", *Electron. Lett.*, Vol. 35, No. 14, pp. 1163-1165, 1999.
- [5] M. Rossetti, P. Bardella and I. Montrosset, "Modeling passive mode-locking in quantum-dot lasers: a comparison between a finite-difference traveling-wave model and a delayed differential equation approach", *IEEE J. Quantum Electron.* Vol. 47, No. 5, pp. 569-576, 2011.
- [6] A. G. Vladimirov and D. Turaev, "Model for passive mode – locking in semiconductor lasers", *Phys. Rev. A*, Vol. 72, No. 3, pp. 033808 – 1 – 033808 – 13, 2005.
- [7] A. G. Vladimirov, D. Turaev and G. Kozyreff, "Delay differential equations for mode – locked semiconductor lasers", *Opt. Lett.* Vol. 29, No. 11, pp. 1221 – 1223, 2004.
- [8] R. Raghunathan, M. T. Crowley, F. Grillot, Y. Li, J. K. Mee, V. Kovanis, and L. F. Lester, "Pulse Characterization of Passively Mode-Locked Quantum-Dot Lasers Using a Delay Differential Equation

Model Seeded With Measured Parameters," *IEEE J. Sel. Topics Quantum Electron.*, Vol. 19, No.4, p. 1100311, 2013.

- [9] R. Raghunathan, "Theoretical and experimental investigation of nonlinear dynamical trends of passively mode-locked quantum dot lasers." *Phd Thesis*, University of New Mexico, 2013.
- [10] Mindaugas Radziunas, Andrei G. Vladimirov, Evgeny A. Viktorov, Gerrit Fiol, Holger Schmeckeber, and Dieter Bimberg, "Pulse broadening in quantum-dot mode-locked semiconductor lasers: simulation, analysis, and experiments", *IEEE J. Quantum Electron.*, Vol. 47, No. 7, July. 2011.
- [11] Radziunas, Mindaugas, Andrei G. Vladimirov, and Evgeny A. Viktorov. "Traveling wave modeling, simulation, and analysis of quantum-dot mode-locked semiconductor lasers." In *SPIE Photonics Europe*, pp. 77200X-77200X. *International Society for Optics and Photonics*, 2010.